

Estimation of the Likelihood of Capacitive Coupling Noise

Sarma B. K. Vrudhula^{*}
ECE Dept., Univ. of Arizona
Tucson, AZ
sarma@ece.arizona.edu

David Blaauw^{† ‡}
EECS Dept., Univ. of Michigan
Ann Arbor, MI
blaauw@ece.umich.edu

Supamas Sirichotiyakul[†]
Sun Microsystems
Boston, MA
supamas@sun.com

Categories and Subject Descriptors

B.7.2 [Hardware]: Integrated Circuits—*Design Aids, Reliability and Testing*

General Terms

Performance, Reliability, Verification

Keywords

Noise, Signal Integrity, Deep Submicron

ABSTRACT

The corruption of signals due to capacitive and inductive coupling of interconnects has become a significant problem in the design of deep submicron circuits (DSM). Noise simulators, based on worst-case assumptions, are overly pessimistic. As a result, when they are used on industrial ICs with hundreds of thousands of nets, thousands of nets are reported as having potential noise violations. There is a need to prioritize the problem nets based on the likelihood of the noise and possibly even eliminate them from further consideration if the likelihood is *negligible*. In this paper, a probabilistic approach is described which allows for a quantitative means to prioritize nets based on the likelihood of the reported noise violation. We derive upper bounds on the probability that the total noise injected on a given victim net by a specific set of aggressors exceeds a threshold. This bound is then used to determine a lower bound on the *expected number of clock cycles* (ENC) before the first *violation* occurs on a given net. Nets can be prioritized based on the ENC. We demonstrate the utility of this approach through experiments carried out on a large industrial processor design using a state-of-the-art industrial noise analysis tool. A significant and interesting

^{*}Work done while on sabbatical with Advanced Design Tools group at Motorola, Austin TX. Also supported by NSF Center for Low Power Electronics (CLPE) (NSF Grant No. EEC-9523338, State of Arizona and Industrial consortium).

[†]Formerly with Advanced Design Tools group at Motorola, Austin TX.

[‡]Supported by SRC grant 2001-HJ-959

Permission to make digital or hard copies of all or part of this work for personal or classroom use is granted without fee provided that copies are not made or distributed for profit or commercial advantage and that copies bear this notice and the full citation on the first page. To copy otherwise, to republish, to post on servers or to redistribute to lists, requires prior specific permission and/or a fee.

DAC 2002, June 10-14, 2002, New Orleans, Louisiana, USA.

Copyright 2002 ACM 1-58113-461-4/02/0006 ...\$5.00.

result of this work is that a substantial portion (25%) of the nets were found to have an ENC of more than five years. If five years is deemed to be sufficiently long time, then these could be eliminated from further consideration.

1. INTRODUCTION

A frequent cause of signal corruption in DSM circuits is capacitive and inductive coupling of interconnects [2, 5, 6, 8, 14, 16]. Their effects can lead to a malfunction of the circuit or degrade its performance. *Functional noise* refers to the situation where a glitch occurs on an otherwise stable net (victim) due to switching of its neighboring nets (aggressors), and propagates to a storage element or a dynamic node, possibly altering its state. *Delay noise* occurs when the victim net is also switching, and can lead to a significant increase in the delay *uncertainty* [2]. This would translate into a reduced clock frequency. The impact of signal interference due to interconnect coupling has become quite significant, and therefore techniques for estimating its magnitude and methods for reducing its effects are critical for the design of DSM circuits [1, 4, 5, 7, 9, 10, 12, 13, 15, 17]. An excellent summary of DSM design issues appears in [16].

Noise analysis tools are designed to be pessimistic due to the consequences of missing a potential malfunction. In large industrial designs, this results in hundreds or even thousands of reported violations, which would be too expensive to fix in terms of chip area, performance and design time. Often the number of aggressors with significant coupled noise can be large, exceeding 5 to 10 aggressors. In such a case, the likelihood of a worst-case composite noise, where all aggressors are required to switch at exactly the right time, is small. Logic correlations and timing windows have been used to reduce the pessimism in noise analysis [3, 7, 10, 13]. In general, only a limited number of logic implications can be derived due to the high computational cost. Moreover, for noise analysis, logic correlations have not been very effective since the relation between *physical proximity* and *logical dependence* gets weaker as circuit sizes increase due to a larger number of globally routed nets. Timing intervals, obtained from static timing analysis, can also be used to identify aggressors that cannot inject noise on the victim net simultaneously. In practice, the intervals are too wide and eliminate only a small portion of the reported noise violations.

In this paper, we present a method that will allow designers to prioritize the potential noise violations based on their likelihood of occurrence. If this likelihood is sufficiently small, it is possible that even during operation of the part for a number of years, the probability of a noise violation on the net is negligible, and the net can be assigned a lower priority for the application of noise avoidance strategies or even eliminated from further consideration. The proposed method is based on estimating the probability that

the noise on a victim will exceed a given threshold. This is used to prioritize nets based on the expected number of clock cycles (ENC) before the first violation occurs on a specific victim. Based on this, a net with a reported noise violation can be assigned a lower priority if its ENC exceeds say, five years or ten years.

In Section 2 a description of the noise waveforms is presented. Sections 3 and 4 contain the main technical contribution, namely the upper bounds on the tail probabilities and estimates of ENC. Results of experiments carried out on a large, high performance PowerPC microprocessor are presented in Section 5.

2. A PROBABILISTIC MODEL OF NOISE

The focus here is on *functional noise* and hence, without loss of generality, we assume that the victim is stable at logic 0, and an aggressor switches from logic 0 to logic 1. A victim with a set of n aggressors will be referred to as a *cluster of size n* . As in the case with most other work on noise analysis, we assume *linearity*, i.e., the composite noise waveform is obtained by taking the sum of the noise waveforms resulting from each aggressor. The general form of the noise waveform seen on a victim due to an aggressor switching is a sum of weighted, decaying exponentials, the number of terms being equal to the order of the circuit. To simplify the algebraic work, we take a linear approximation for the *rising* and *falling* portions of the waveform and consequently, the noise waveform resulting from each aggressor is approximated by a triangular pulse. In the interest of being conservative one can construct a triangular pulse that is an envelope of a given exponential pulse, i.e. contains most of the exponential pulse.

Associated with each aggressor i , is a timing interval $[a_i, b_i]$ (obtained from static timing analysis), where a_i and b_i denote the earliest and latest possible arrival times of the transition. Thus, the noise waveform resulting from aggressor i , which is denoted by $Z_i(t)$, is represented by $(h_i, r_i, d_i, a_i, b_i)$, where h_i is the peak noise voltage and r_i and d_i are the slopes of the rising and falling edges of the noise waveform, respectively.

The *randomness* or variability of the noise on a victim net is over different clock cycles and arises due to the fact that an aggressor may or may not switch during a clock cycle, as well as the time when an aggressor switches over its interval. Let τ_i be the random variable that denotes the time instance in $[a_i, b_i]$ at which aggressor i switches. We assume that τ_i is uniformly distributed over $[a_i, b_i]$, i.e.,

$$F_{\tau_i}(x) = \text{Prob}(\tau_i \leq x) = \frac{(x - a_i)_+ - (x - b_i)_+}{b_i - a_i}, \quad (1)$$

where $(x)_+ = x$ if $x \geq 0$, otherwise $(x)_+ = 0$. In the absence of any other information, the uniform distribution is the meaningful choice. However, this assumption is not very restrictive and the approach can be extended to other distributions of switching events, e.g., the triangular distribution. For a given value of τ_i , $Z_i(t)$ is expressed as

$$Z_i(t) = \begin{cases} r_i(t - \tau_i) & \tau_i \leq t \leq \tau_i + \frac{h_i}{r_i} \\ d_i(\frac{h_i}{r_i} - (t - \tau_i)) + h_i & \tau_i + \frac{h_i}{r_i} \leq t \leq \tau_i + \frac{h_i}{r_i} + \frac{h_i}{d_i} + \tau_i \\ 0 & \text{elsewhere.} \end{cases} \quad (2)$$

With τ_i being a random variable, $Z_i(t)$ is a stochastic process, and for a fixed value of t , $Z_i(t)$ is a random variable. Let $F_{Z_i(t)}(z) = \text{Prob}(Z_i(t) \leq z)$ denote the distribution function of $Z_i(t)$. For a fixed value of t , if N waveforms given by (2) are generated corresponding to N sample observations of τ_i , then $F_{Z_i(t)}(z)$ represents the fraction

of those N waveforms that at time t have a value $\leq z$. For a fixed t ,

$$\{Z_i(t) \leq z\} = \{\tau_i \geq t - \frac{z}{r_i}\} \cup \{\tau_i \leq t - \frac{h_i}{r_i} - \frac{h_i}{d_i} + \frac{z}{r_i}\}. \quad (3)$$

This leads directly to the distribution function of $Z_i(t)$, expressed in terms of the distribution function of τ_i .

$$F_{Z_i}(z) = \begin{cases} 1 - F_{\tau_i}(t - \frac{z}{r_i}) + F_{\tau_i}(t - \frac{h_i}{r_i} - \frac{h_i}{d_i} + \frac{z}{r_i}) & 0 \leq z \leq h_i \\ 1 & z \geq h_i \\ 0 & \text{otherwise.} \end{cases} \quad (4)$$

Let $S_n(t)$ represent the waveform of the total noise on a given victim net in a cluster of size n . As stated earlier, the use of linear models for the victim and aggressor drivers, allows us to represent the total noise on a victim as a sum of the noise due to each aggressor. We assume that the random variables $Z_i(t)$, $i = 1, 2, \dots, n$, are independent. Under the zero delay model, the determination of logic correlations (which is an intractable problem in itself) is done separately and only those aggressors that would be switching in the same direction would be included in a cluster. These have been accounted for in the experiments. However, temporal correlations are far more difficult to model and no effective solution to include them and still maintain analytical tractability is known. To account for the fact that an aggressor may or may not switch within a clock period, we introduce a binary random variable X_i associated with aggressor i , where $X_i = 1$ with probability p_i and $X_i = 0$ with probability $(1 - p_i)$. p_i is called the switching probability of aggressor i . The random variable that represents the total noise on the victim is:

$$S_n(t) = Z_1(t) * X_1 + Z_2(t) * X_2 + \dots + Z_n(t) * X_n. \quad (5)$$

3. CRITERION FOR PRIORITIZING NETS

A simple criterion that designers can use to prioritize nets that are identified as having potential noise violations is the *expected* number of clock cycles (ENC) before the first violation occurs. A noise violation is said to occur on a victim net if the total noise $S_n(t)$ on that victim exceeds a given threshold α . The threshold is calculated based on the characteristics of the victim's receiver gate. On each clock cycle, we observe a realization of $S_n(t)$. Let the random variable $N(t)$ denote the number of clock cycles required to observe the first noise violation at time t . Assuming independence of noise waveforms over different clock cycles, the probability that the noise on this victim will exceed α for the first time on k th cycle is given by

$$\text{Prob}(N(t) = k) = [P(S_n(t) \leq \alpha)]^{k-1} * (1 - P(S_n(t) \leq \alpha)). \quad (6)$$

Let \mathcal{E} denote the expectation operator. The expected number of clock cycles before the first violation occurs at time t within a clock period, is given by

$$\text{ENC}(t) = \mathcal{E}(N(t)) = \frac{1}{P(S_n(t) > \alpha)}. \quad (7)$$

When assigning a victim net a very low priority or even discarding it from further consideration because its $\text{ENC}(t)$ is very large (e.g. 5 years), we should ensure that t is selected so that at no other value of t , the $\text{ENC}(t)$ is smaller. Thus we have

$$t^* = \{t \mid \text{ENC}(t) \text{ is minimum}\} \quad (8)$$

$$\text{ENC}^* = \text{ENC}(t^*). \quad (9)$$

To compute ENC(t), we need the distribution function of $S_n(t)$. An analytical form does not appear to be possible. The alternative, which is to carry out numerical convolution for each t , would be computationally prohibitive. Therefore, we proceed with the next best alternative, which is to derive bounds on $P(S_n(t) > \alpha)$.

4. BOUNDS ON NOISE PROBABILITY

A common strategy to construct an upper bound on the probability that a non-negative random variable exceeds a given value is to construct a parametric family of upper bounds and then find the value of the parameter that minimizes the upper bound. This approach is based on the Chernoff bound [11], which states that

$$P(S_n(t) > \alpha) \leq e^{-\theta\alpha} \Phi_{S_n(t)}(\theta) \quad \forall \theta \geq 0, \quad (10)$$

where $\Phi_{S_n(t)}(\theta)$ is the moment generating function (mgf) of $S_n(t)$, and θ is an unknown parameter to be determined. From Equation 5 and from the properties of the mgf, we have

$$\Phi_{S_n(t)}(\theta) = \prod_{i=1}^n (p_i \Phi_{Z_i(t)}(\theta) + 1 - p_i). \quad (11)$$

By definition of the mgf, we have

$$\Phi_{Z_i(t)}(\theta) = \sum_{k=0}^{\infty} \frac{\mathcal{E}(Z_i^k(t)) \theta^k}{k!}. \quad (12)$$

Let $B(\theta, t, \alpha) = e^{-\theta\alpha} \Phi_{S_n(t)}(\theta)$. The value of θ that minimizes $B(\theta, t, \alpha)$ is the solution to the equation [11]

$$\frac{\mathcal{E}(S_n(t) e^{\theta S_n(t)})}{\mathcal{E}(e^{\theta S_n(t)})} = \frac{\Phi'_{S_n(t)}(\theta)}{\Phi_{S_n(t)}(\theta)} = \alpha. \quad (13)$$

Equation (13) can be simply expressed as

$$\frac{d \log(\Phi_{S_n(t)}(\theta))}{d\theta} = \alpha. \quad (14)$$

Using (11) and (14), the value of θ that minimizes the bound given by the RHS of (10) is the solution to the equation

$$\sum_{i=1}^n \frac{p_i \Phi'_{Z_i(t)}(\theta)}{p_i \Phi_{Z_i(t)}(\theta) + 1 - p_i} = \alpha. \quad (15)$$

We have now established a method to compute a lower bound on ENC. First, we have to determine t^* (see (8)). Then we have to minimize $B(\theta, t^*, \alpha)$ with respect to θ . Before we proceed with this task, we need expressions for $\mathcal{E}(Z_i^k(t))$ (see Equations 11 and 12).

4.1 Moments of Total Noise

By definition, $\mathcal{E}(Z_i^k(t)) = \int_{-\infty}^{\infty} z^k dF_{Z_i(t)}(z)$ and $F_{Z_i(t)}(z)$ is given by (1). Integrating by parts and noting that $F_{Z_i(t)}(z)$ has a finite jump at $z = 0$, we obtain the following recurrence relation.

$$\mathcal{E}(Z_i^k(t)) = h_i^k - k \int_0^h z^{k-1} F_{Z_i(t)}(z) dz. \quad (16)$$

Equation (16) can be solved exactly. The result is

$$\begin{aligned} \mathcal{E}(Z_i^k(t)) = & 0^k F_{Z_i(t)}(0) + \\ & \frac{1}{(b_i - a_i)(k+1)! r_i} \left[(h_i + r_i(t - b_i - h_i/r_i)_+)^{k+1} - \right. \\ & (h_i + r_i(t - a_i - h_i/r_i)_+)^{k+1} + \\ & \left. (r_i(t - a_i)_+)^{k+1} - (r_i(t - b_i)_+)^{k+1} \right] + \\ & \frac{1}{(b_i - a_i)(k+1)! d_i} \left[(h_i - d_i(t - b_i - h_i/r_i)_+)^{k+1} - \right. \\ & (h_i - d_i(t - a_i - h_i/r_i)_+)^{k+1} + \\ & \left. (-d_i(t - a_i - h_i/r_i - h_i/d_i)_+)^{k+1} - \right. \\ & \left. (-d_i(t - b_i - h_i/r_i - h_i/d_i)_+)^{k+1} \right], \end{aligned} \quad (17)$$

where $F_{Z_i(t)}(0)$ (using (4) and (1)) is given by

$$\begin{aligned} F_{Z_i(t)}(0) = & 1 - \frac{1}{b_i - a_i} [(t - a_i)_+ - (t - b_i)_+] + \\ & \frac{1}{b_i - a_i} \left[\left(t - \left(\frac{h_i}{r_i} + \frac{h_i}{d_i} + a_i \right)_+ \right) - \left(t - \left(\frac{h_i}{r_i} + \frac{h_i}{d_i} + b_i \right)_+ \right) \right]. \end{aligned}$$

Equation (17) expresses the k th order moment of the noise waveform due to aggressor i , in terms of its descriptors, $(h_i, r_i, d_i, a_i, b_i)$. The moments of $S_n(t)$ can be obtained from Equations 17 and 5. To see how the theoretical and sample moments compare, the first four moments were computed for many clusters taken from a PowerPC microprocessor. Using the timing intervals for each aggressor that were obtained from static timing analysis, and the noise estimates produced by the simulator [10], a MonteCarlo simulation was carried out by varying the switching point of each aggressor. For each selection of switching points, the composite waveform was computed, and this was repeated 5000 times. This corresponds to 5000 clock cycles. Figures 1 and 2 show plots of the theoretical (using Equation (17)) and sample mean, and standard deviation. The timing intervals associated with each aggressor are shown at the bottom of each plot. There is also equally good agreement between the higher order theoretical and sample moments.

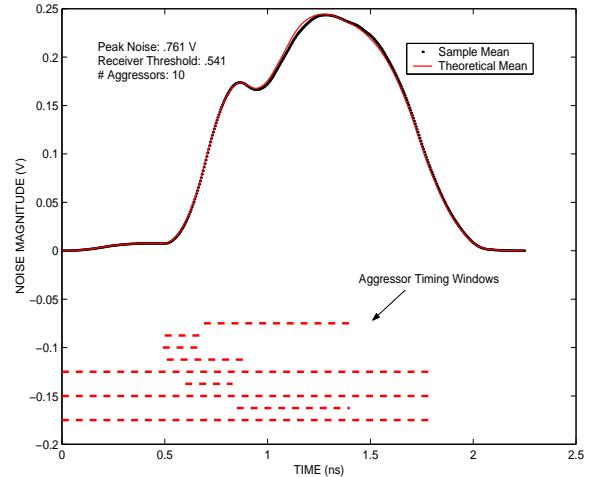


Figure 1: Theoretical and Sample Mean of Total Noise of one victim with 10 aggressors

Since the ordinary moments involve only simple powers of t , the mgf $\Phi_{Z_i(t)}(\theta)$ can be obtained almost by inspection. Using the

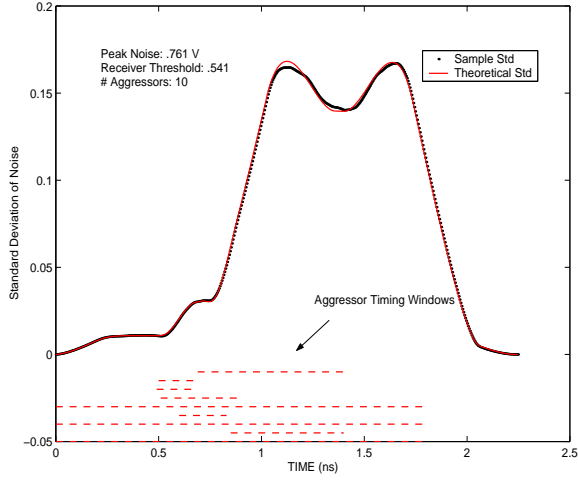


Figure 2: Theoretical and Sample Std. of Total Noise of one victim with 10 aggressors

definition of $\Phi_{Z_i(t)}(\theta)$ given in (12) and substituting the expression for $\mathcal{E}(Z_i^k(t))$ given in (17) into (12), we obtain

$$\begin{aligned} \Phi_{Z_i(t)}(\theta) = & F_{Z_i(t)}(0) + \\ & \frac{1}{(b_i - a_i)r_i\theta} [\exp(\theta(h_i + r_i(t - b_i - h_i/r_i)_+)) \\ & - \exp(\theta(h_i + r_i(t - a_i - h_i/r_i)_+)) + \\ & \exp(\theta r_i(t - a_i)_+) - \exp(\theta r_i(t - b_i)_+)] + \\ & \frac{1}{(b_i - a_i)d_i\theta} [\exp(\theta(h_i + d_i(t - b_i - h_i/r_i)_+)) \\ & - \exp(\theta(h_i + d_i(t - a_i - h_i/r_i)_+)) + \\ & \exp(-\theta d_i(t - (h_i/r_i + h_i/d_i + a_i)_+)) - \\ & \exp(-\theta d_i(t - (h_i/r_i + h_i/d_i + b_i)_+))]. \end{aligned} \quad (18)$$

$\Phi_{S_n(t)}(\theta)$ (the mgf of $S_n(t)$) is computed by substituting Equation (18) into Equation (11).

Figures 3 and 4 show plots of the bound in (10) for a cluster of size 10, without and with timing intervals, respectively. Note that ignoring the timing intervals of aggressors simply means that the timing intervals span the entire clock period. Figures 5 and 6 show that the bound (10) as a function of θ in the interval of interest. From these plots, it is clear that once the desired value of t is obtained, then the optimal value of θ can be obtained very quickly by either gradient or direct search techniques.

4.2 Determining t^*

In Section 3 we stated that a lower bound on the expected number of clock cycles to observe the first violation (total noise exceeding a given threshold) requires determining a value of t at which $\text{ENC}(t)$ is minimum, or equivalently the value of t that maximizes $B(\theta, t, \alpha)$. That value of t is denoted by t^* . Since θ is also unknown, an iterative search along θ and t would be very time consuming, and prohibitively so, given the large number of clusters that have to be processed. Moreover, convergence is not guaranteed. We now describe a procedure that identifies t^* first without having to know θ and then the bound $B(\theta, t^*, \alpha)$ can be easily minimized with respect to θ using gradient search.

The solution to finding t^* is based on the monotonicity proper-

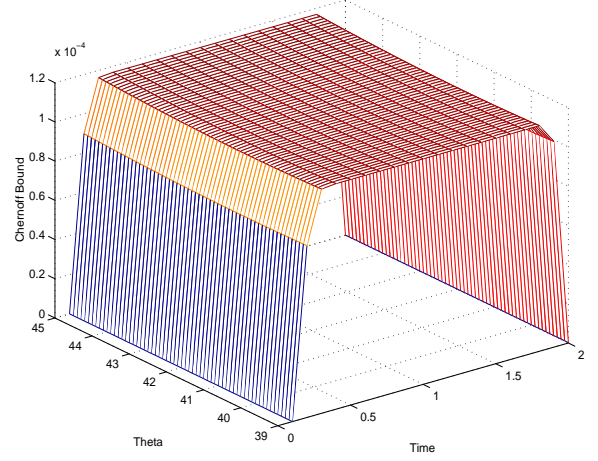


Figure 3: Chernoff Bound of a Net with 10 aggressors without timing intervals.

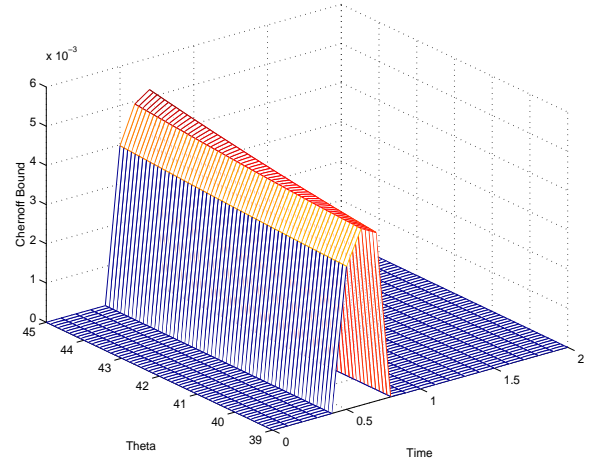


Figure 4: Chernoff Bound of a Net with 10 aggressors with timing intervals.

ties of the mgf $\Phi_{Z_i(t)}(\theta)$. These properties allow us to identify a finite set ($4n$ for a cluster of size n) of distinguished time points \mathcal{T} , which we refer to as *breakpoints*. Now for a fixed θ , the maximum value of $\Phi_{S_n(t)}(\theta)$ will occur at the breakpoints or in between two breakpoints. The latter may occur because at some breakpoint, the mgf of some of the aggressors are increasing, while the mgf of others are decreasing. In such a situation, we would have to iteratively search, between every pair of such breakpoints, for the value of t where $\Phi_{S_n(t)}(\theta)$ attains a maximum. Moreover, the point within such an interval where the maximum of $\Phi_{S_n(t)}(\theta)$ occurs will generally depend on θ . To avoid this, we construct a modified mgf $\tilde{\Phi}_{S_n(t)}(\theta)$ such that $\tilde{\Phi}_{S_n(t)}(\theta) \geq \Phi_{S_n(t)}(\theta)$, for all θ , and so that only the breakpoints in \mathcal{T} need to be examined in order to determine the value of t where $\tilde{\Phi}_{S_n(t)}(\theta)$ is maximum. Furthermore, many of the points in \mathcal{T} can be discarded. Finally, at each time point in the reduced set of breakpoints, we solve (15) to find θ using gradient search and choose that value of θ that minimizes the bound. Note

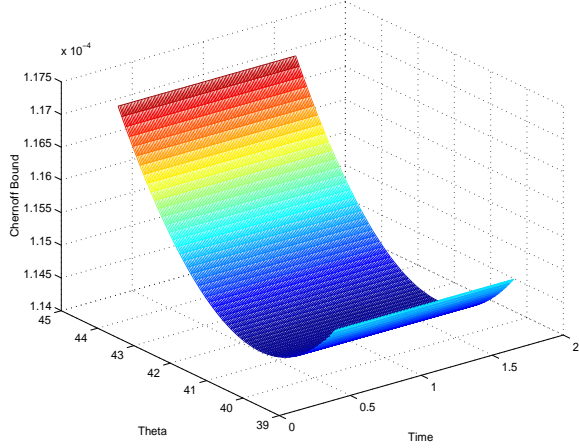


Figure 5: Plot in Figure 3 restricted to smaller range of t .

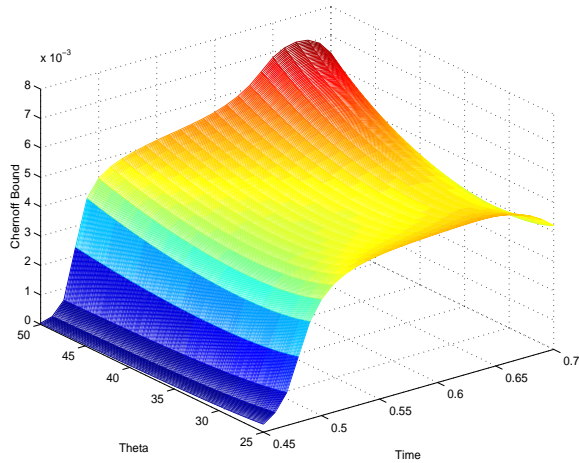


Figure 6: Plot in Figure 4 restricted to smaller range of t .

that this is a conservative solution in that it will lead to a smaller lower bound on ENC^* .

Consider the mgf of $Z_i(t)$ given in (18). For a fixed θ , its behavior as a function of t can be classified into two cases.

Case 1. $b_i - a_i \geq h_i/r_i + h_i/d_i + a_i$. This situation occurs when the width of the timing interval is greater than the width of the noise pulse. In this case, $\Phi_{Z_i(t)}(\theta)$ is

- monotonically increasing for $t \in [a_i, h_i/r_i + h_i/d_i + a_i]$,
- constant for $t \in [h_i/r_i + h_i/d_i + a_i, b_i]$, and
- monotonically decreasing for $t \in [b_i, h_i/r_i + h_i/d_i + b_i]$.

Case 2. $b_i - a_i < h_i/r_i + h_i/d_i$. In this case, $\Phi_{Z_i(t)}(\theta)$ is

- monotonically increasing for $t \in [a_i, \tilde{t}_i]$, and
- monotonically decreasing for $t \in [\tilde{t}_i, h_i/r_i + h_i/d_i + b_i]$,

where \tilde{t}_i is given by

$$\tilde{t}_i = \frac{d_i}{r_i + d_i} \left(\frac{h_i}{r_i} + \frac{h_i}{d_i} + a_i \right) + \frac{r_i}{r_i + d_i} b_i. \quad (19)$$

The points where $\Phi_{Z_i(t)}(\theta)$ changes direction are the *breakpoints* of $Z_i(t)$. The breakpoints of all the aggressors are collected into a list \mathcal{T} and sorted in increasing order. Formally, $\mathcal{T} = \cup_i \tau_i$, where τ_i is defined as

$$\tau_i = \begin{cases} \left\{ a_i, \frac{h_i}{r_i} + \frac{h_i}{d_i} + a_i, b_i, \frac{h_i}{r_i} + \frac{h_i}{d_i} + b_i \right\} & \text{if case 1} \\ \left\{ a_i, \tilde{t}_i, \frac{h_i}{r_i} + \frac{h_i}{d_i} + b_i \right\} & \text{otherwise.} \end{cases}$$

With n aggressors, the maximum possible number of points in \mathcal{T} is $4n$. However, most of the points in \mathcal{T} can be eliminated from further consideration. This is done by associating a direction $\delta_{i,j}$ with $\Phi_{Z_i(t_j)}(\theta)$ for each $t_j \in \mathcal{T}$.

$$\delta_{i,j} = \begin{cases} -1 & \text{if } \Phi_{Z_i(t_j)}(\theta) \text{ is decreasing} \\ 0 & \text{if } \Phi_{Z_i(t_j)}(\theta) \text{ is constant} \\ 1 & \text{if } \Phi_{Z_i(t_j)}(\theta) \text{ is increasing.} \end{cases}$$

Now $\tilde{\Phi}_{Z_i(t)}(\theta)$ can be constructed from $\Phi_{Z_i(t)}(\theta)$ as follows. Let $\mathcal{T} = \{t_1, t_2, \dots, t_m\}$.

$$\begin{aligned} \tilde{\Phi}_{Z_i(t_1)}(\theta) &= \Phi_{Z_i(t_1)}(\theta) \\ \tilde{\Phi}_{Z_i(t_j)}(\theta) &= \begin{cases} \Phi_{Z_i(t_{j-1})}(\theta) & \text{if } \delta_{i,j-1} = -1, \\ & \text{and } \exists k, \delta_{k,j-1} = 1 \\ \Phi_{Z_i(t_j)}(\theta) & \text{otherwise} \end{cases} \end{aligned}$$

and $\tilde{\Phi}_{S_n(t)}(\theta) = \prod_{i=1}^n \tilde{\Phi}_{Z_i(t)}(\theta)$.

As stated above, many of the points in \mathcal{T} can be discarded. Let t_j be the first point in \mathcal{T} such that $\delta_{i,j} = -1$, for some i . Let t_k be the last point in \mathcal{T} such that $\delta_{i,k} = 1$, for some i . Then points in (t_1, \dots, t_{j-1}) and (t_{k+2}, \dots, t_m) can be discarded. This is because, t_j and t_k are the first and last points where one of the modified mgfs $\tilde{\Phi}_{Z_i(t)}(\theta)$ has reached its peak. Note that this reduction is possible only with $\tilde{\Phi}_{Z_i(t)}(\theta)$ and not with $\Phi_{Z_i(t)}(\theta)$. Once a time point $t^* \in \mathcal{T}$ where $\tilde{\Phi}_{S_n(t)}(\theta)$ is maximum is identified, then the value of θ that minimizes $\tilde{B}(\theta, t^*, \alpha)$ is computed by numerically solving (15) with $\tilde{\Phi}$ replacing Φ .

5. EXPERIMENTAL RESULTS

The experimental results reported in this paper were generated by performing noise analysis for a high performance microprocessor. The noise simulator, called ClariNet [10], was developed to analyze large, high performance processor designs. It embodies several features that help speedup noise analysis, allowing it to process hundreds of thousands of nets in a few hours. The total number of nets analyzed were nearly 200,000. Each net was analyzed twice - once for *low overshoot* (victim net is to be stable at logic 0 and its aggressors switch from logic 0 to logic 1) and once for *high undershoot* (victim net is stable at logic 1 and aggressors switch from logic 1 to logic 0). As a result, the total number of violations was 2501. Although the cluster size (number of aggressors per victim) can be quite large, the number that contributed a significant amount of noise was found to be less than 10. For this reason, we set the maximum cluster size to 10. For each net, the noise report indicates the peak height and width of the noise injected on the net by each aggressor, and the threshold of the receiver gate. This is data that was used for the probabilistic analysis as described in this paper.

For each cluster, the optimal value of the bound was computed, with α set to the receiver's threshold. Of the 2501 reported violations, 634 or 25.35% of them had an expected number of clock cycles for the first violation exceeding 5 years for a continuously running 555 MHz processor. If 5 years is an acceptable level then

these can be eliminated from further consideration. Figure 7 shows a plot of the percentage of nets that have an ENC greater than or equal to the value on the abscissa. It is important to note that the set of all nets when using timing intervals (lower plot in Figure 7) is much smaller than the set of nets when timing intervals are ignored.

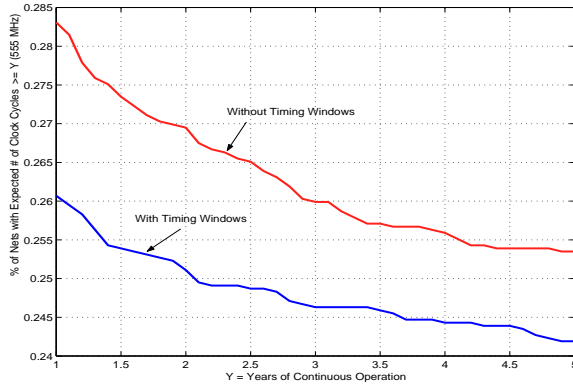


Figure 7: Expected # of Clock Cycles for 1st Violation

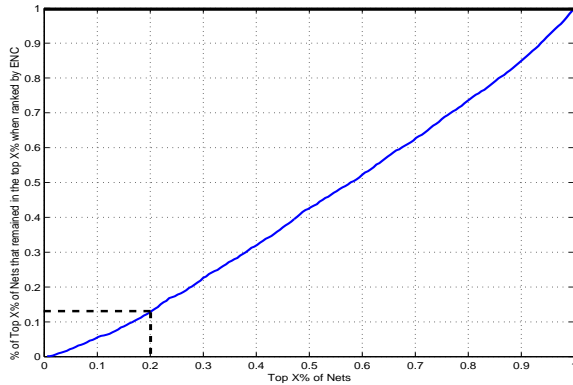


Figure 8: Ranking Nets by Peak Noise and ENC

Next we deleted the nets whose ENC was greater than or equal to 5 years. The number of nets remaining was 1867. For these nets, we computed the ENC* values. This provides an alternative ranking based on the expected number of clock cycles required to observe a noise violation for the first time, rather than simply the sum of all the noise peaks injected by each aggressor. Two sorted lists L_{PEAK} and L_{ENC} of the nets were generated. L_{PEAK} is the set of nets in decreasing order of the magnitude of the peak noise of the composite waveform. L_{ENC} is the set of nets in increasing order of their ENC* values. Figure 8 shows a plot of the percentage of nets in the original list L_{PEAK} that retain their ranking in the second list L_{ENC} , as each list is traversed. The abscissa represents the top X% of the nets. The ordinate represents the percentage of the nets in the top X% of list L_{PEAK} that remained in the top X% of the nets in list L_{ENC} . For example, from the top 20% of the list L_{PEAK} which represents 373 nets, only 12.5% of them (≈ 46 nets) remained in the top 20% of L_{ENC} . If the ranking of the nets did not change then the plot would be a horizontal line at 1. The important conclusion here that the probabilistic approach identifies nets based not only on the noise magnitude but also on the likelihood of occurrence. Nets for which the simulator reports a relatively small noise violation may become more important, resulting in corrective action being

taken on them before nets with larger noise magnitudes.

6. CLOSING REMARKS

In this paper we presented an approach to analyzing functional noise. The objective was to use estimates of the probability that the noise will exceed a specified threshold as a means to prioritize nets or even eliminate them from further consideration if the likelihood is small. Results of experiments carried out on a large industrial high performance microprocessor, using a recently developed state-of-the-art noise simulator were also presented.

7. REFERENCES

- [1] R. Arunachalam, K. Rajagopal, and L. T. Pileggi. TACO: Timing Analysis with Coupling. In *Proc. ICCAD*, pages 1–8, Nov. 1998.
- [2] Y. Cao, T. Sato, X. Huang, C. Hu, and D. Sylvester. New Approaches to Noise-Aware Static Timing Analysis. In *Proc. TAU*, pages 8–13, Dec. 2000.
- [3] P. Chen and K. Keutzer. Towards True Crosstalk Noise Analysis. In *Proc. ICCAD*, pages 132–137, Nov. 1999.
- [4] J. Cong, D. Z. Pan, and P. V. Srinivas. Improved Crosstalk Modeling for Noise Constrained Interconnect Optimization. In *Proc. TAU*, pages 14–20, Dec. 2000.
- [5] A. Devgan. Efficient Coupled Noise Estimation for On-Chip Interconnects. In *Proc. ICCAD*, pages 147–151, Nov. 1997.
- [6] K. Gala, V. Zolotov, R. Panda, B. Young, J. Wang, and D. Blaauw. On-Chip Inductance Modeling and Analysis. In *Proc. DAC*, pages 63–68, June 2000.
- [7] A. Glebov, S. Garrilov, D. Blaauw, S. Sirichotiyakul, C. Oh, and V. Zolotov. False-Noise Analysis using Logic Implications. In *Proc. ICCAD*, pages 515–521, Nov. 2001.
- [8] H. Hu and S. Sapatnekar. Circuit-Aware On-Chip Inductance Extraction. In *Proc. CICC*, 2001.
- [9] A. B. Kahng, S. Muddu, and E. Sarto. Switch Factor Based Analysis of Coupled RC Interconnects. In *Proc. ASIC/SoC Conf.*, pages 3–8, 1999.
- [10] R. Levy, D. Blaauw, G. Braca, A. Dasgupta, A. Grinshpon, C. Oh, B. Orshav, S. Sirichotiyakul, and V. Zolotov. ClariNet: A noise analysis tool for deep submicron design. In *Proc. DAC*, pages 223–238, June 2000.
- [11] J. Proakis. *Introduction to Digital Communications*. McGraw-Hill, New York, 1983.
- [12] S. S. Sapatnekar. On the chicken-and-Egg Problem of Determining the Effect of Crosstalk on Delay in Integrated Circuits. In *Proc. IEEE 8th Topical Meeting on Electrical Performance of Electronic Packaging*, pages 245–248, 1999.
- [13] Y. Sasaki and G. De Michelli. Crosstalk delay analysis using relative window method. In *Proc. ASIC/SoC Conf.*, pages 9–13, 1999.
- [14] K. L. Sheppard and V. Narayanan. Noise in Deep Submicron Digital Design. In *Proc. ICCAD*, pages 524–531, Nov. 1996.
- [15] S. Sirichotiyakul, D. Blaauw, R. Levy, C. Oh, S. Shams, V. Zolotov, and J. Zuo. Driver Modeling and Alignment of Worst-Case Delay Noise. In *Proc. TAU*, pages 1–7, Dec. 2000.
- [16] D. Sylvester and K. Keutzer. Getting to the Bottom of Deep Submicron. In *Proc. ICCAD*, pages 203–211, Nov. 1998.
- [17] A. Vittal, L. H. Chen, M. Marek-Sadowska, K.-P. Wang, and S. Yang. Crosstalk in VLSI Interconnections. *IEEE Trans. on Computer Aided Design*, pages 1817–1824, Dec. 1999.